Microstructure and properties of giant magnetoresistive granular Au80Co20 alloys

Vrenken, H.; Kooi, B. J.; de Hosson, J. Th. M.

Published in:
Journal of Applied Physics

DOI:
10.1063/1.1325381

Publication date:
2001

Microstructure and properties of giant magnetoresistive granular $Au_{80}Co_{20}$ alloys

H. Vrenken, B. J. Kooi, and J. Th. M. De Hosson[a)]
Department of Applied Physics, Materials Science Center and the Netherlands Institute for Metals Research, Nijenborgh 4, 9747 AG Groningen, The Netherlands

(Received 11 July 2000; accepted for publication 21 September 2000)

The relationship between microstructure and giant magnetoresistance (GMR) of granular $Au_{80}Co_{20}$ was investigated. Two different processing routes were explored. With the melt spinning technique the microstructure appeared to be so coarse that it was not expected to exhibit any substantial GMR effect. On the other hand, with the procedure of solid-solution annealing and water quenching afterwards, a suitable nanostructure was prepared that showed a GMR of 29% at 10 K and 50 kOe. Subsequent annealing causes coarsening of Co particles. In additional spinodal decomposition occurred for a certain temperature range and a loss of coherency of the Co particles with respect to the Au was observed with high-resolution transmission energy microscopy. At magnetic fields above ~20 kOe, all annealed alloys showed a saturating magnetization, whereas the resistance is still steadily decreasing, challenging the presumed mathematical relationship between GMR and overall magnetization. © *2001 American Institute of Physics.* [DOI: 10.1063/1.1325381]

I. INTRODUCTION

Since 1992 an impressive decrease in the electric resistance upon applying a magnetic field, the so-called giant magnetic resistance (GMR), has been know to occur in granular alloys.[1,2] Although considerable information on the phenomenon has been obtained, a comprehensive theory is not designed yet. Some models were proposed linking the GMR effect to the overall magnetization and/or the average magnetic particle size.[3–5] The experimental data on $Au_{80}C_{20}$ presented and discussed in this article consisting of high-resolution transmission electron microscopy (HRTEM), observations together with MR and magnetization measurements show some intriguing phenomena which are not governed in those models.

The degree of alignment of the magnetic moment of sites at which spin-dependent scattering takes place, determines the reduction of the resistance. The GMR is therefore often presumed to be a mathematical function of the overall magnetization M. In the case of purely superparamagnetic (SPM) behavior, it is supposed to be proportional to M squared.[2,3,6,7] If the behavior is not solely SPM, but the larger particles are ''blocked,'' the model by Wiser[5] and Musa *et al.*[8] provides a functional relationship between the GMR and M that includes terms both linear and quadratic in M. Actually, it is based on the presence of a particle-size distribution with, at any given temperature, the smaller particles being SPM and the larger being blocked. The relative fractions of SPM and blocked particles are temperature dependent. Further, the assumption of independent magnetic moments for the individual SPM particles may fail because of the interaction among particles. This also leads to deviations of the M^2 proportionally, particularly at small values of M.[6,7] At any rate, it is still assumed that the GMR effect can be written as a function of the overall magnetization. This article will show that at least in our Au–Co system and probably in general for granular systems, no meaningful relationship between overall magnetization and the resistance can be established.

By including not only magnetization measurements but also detailed (HR)TEM observations of the structure at a nanometer scale, it is possible to arrive at a more direct relation between the microstructure and GMR properties and to test the predictions of theoretical models to a certain depth. Among others the Au–Co system was chosen because of the contrast in TEM images between Au and Co. The GMR properties of granular Au–Co alloys have been investigated before in a few cases[9,10] but less exhaustive than those of granular Cu–Co alloys. Melt spinning is the commonly known method used to obtain a fine dispersion of Co in Au.[9,10] One research group reported on water quenching of a solid solution of Au–Co.[11] With respect to the Cu–Co the quenching of Au–Co is more critical, since in the latter the driving force for phase separation is much larger. The difference in atomic radius between Au and Co is large, whereas that between Cu and Co is rather small. In this work both routes of melt spinning and of solid-solution quenching were explored, in order to arrive at suitable materials exhibiting GMR. We will show that the technique of solid-solution quenching is superior to that of melt spinning for obtaining the desired nanostructure of Au–Co. Finally, the quenched material was annealed in order to induce growth of the Co particles in Au. The growth was monitored by HR-TEM and its influenced on GMR and magnetization was investigated.

II. EXPERIMENT

Granular alloys of Au and Co, which are suitable for exhibiting GMR, can be prepared by sufficiently suppressing

a)Author to whom correspondence should be addressed; electronic mail hossonj@phys.rug.nl

the decomposition of the two elements into separate phases. An arc furnace was used to prepare a precursor alloy of 80 at. % Au and 20 at. % Co from the (99.99%) pure constituents. The button was cut and cold rolled to a foil. Two methods were employed to arrive at suitable nanostructured material. With melt spinning, using a velocity at the surface of the Cu wheel of about 30 m/s, long ribbons with a width of about 5 mm and a thickness of about 50 μm were produced. The alloy was molten in a quartz nozzle by an induction furnace and blown on the polished Cu wheel by applying a sudden Ar overpressure. An Ar shielding gas was used around the Cu wheel and inside the tube into which the ribbons were ejected to prevent oxidation. The second method consisted of annealed cold-rolled foil (typical thickness 23 μm) for 17 h at 970 °C in an evacuated quartz tube followed by water quenching. From the equilibrium phase diagram of Au–Co it is clear that, at 970 °C, 20 at. % Co can dissolve in the solid Au. Because the alloy is already in the solid state, no latent heat is released upon cooling. So even though the cooling rate is lower than with melt spinning, the nanostructure does not necessarily have to be coarser than with melt spinning. Annealing of the quenched material was performed in evacuated Pyrex tubes at temperatures ranging between 300 and 500 °C for 1 h.

The microstructure of the samples was investigated with a JEOL 4000 EX/II HRTEM operating at 400 kV (spherical aberration coefficient: 0.97 ± 0.02 mm, defocus spread: 7.8 ± 1.4 nm, and beam semiconvergence angle: 0.8 mrad). TEM samples were prepared by ion milling using a Gatan PIPS model 691. We used a Linear Research LR-700 ac resistance bridge[12] for the resistance measurements using a four-point probe configuration. For these measurements, ribbons with a width of about 0.5 mm and a length of 10 mm were cut using a razor blade from the (23 μm thick) foil. A Quantum Design Magnetic Property Measurement System[13] was used for the magnetization measurements.

Assuming that the GMR effect was isotropic for each sample only resistance measurements for a single combination of field, sample, and current orientations were performed. The orientation of the external magnetic field with respect to the sample was kept the same for the resistance and the magnetization measurements.

III. RESULTS

A. HRTEM

The ultimate aim of melt spinning or solid-solution quenching is to suppress completely the decomposition of Co and Au. Then, annealing treatments can be used to arrive at the desired nanostructure with, e.g., a homogeneous and narrow distribution of Co particles with average sizes of a few nanometers. Regarding this objective the microstructure of the melt-spun alloys, i.e., already without annealing, exhibited a much too coarse decomposition. A typical example of the structure obtained is shown in the bright-field TEM image of Fig. 1. Microstructures are present within a certain range: lamella-like structures of thickness of about 20 nm or more, and more or less spherical particles with a diameter up to about 200 nm. All the areas of Co possess the fcc crystal

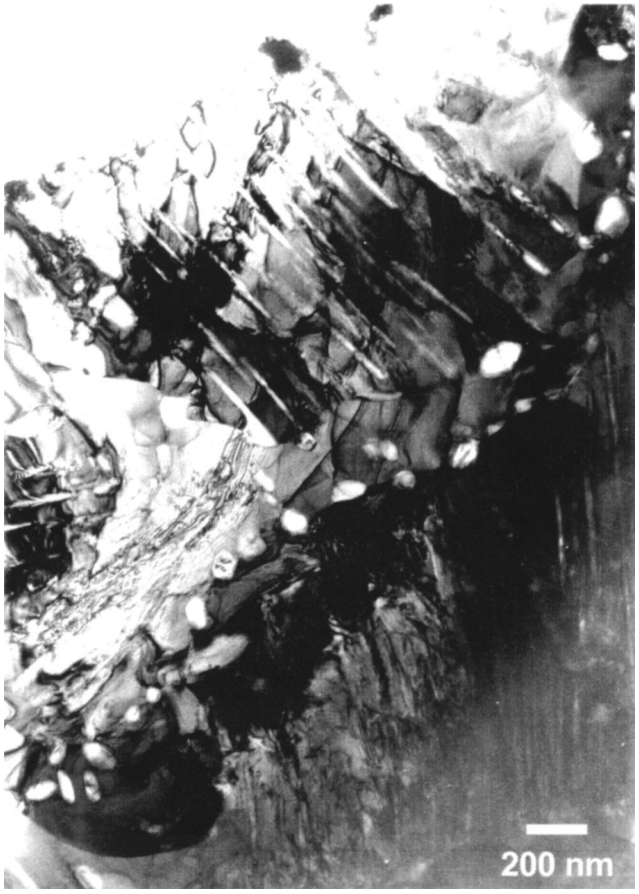

FIG. 1. Bright field TEM image of melt-spun $Au_{80}Co_{20}$. Coarse decomposition is visible.

structure. As a matter of course, the melt-spun structure might still give rise to a (small) GMR effect, but because it deviated too much from our desired microstructure further investigations were abandoned. This view is supported by the relatively small GMR effects of a few percent observed for melt-spun Au–Co alloys previously published.[10]

After a water quench from 970 °C of the solid solution with chemical composition $Au_{80}Co_{20}$ only small facetted Co-rich particles were observed which were homogeneously dispersed in the Au matrix. The HRTEM image shown in Fig. 2, displays this for viewing along the $\langle 110 \rangle$ fcc zone axis. The particles appear somewhat brighter with respect to their surroundings due to the smaller atomic mass of Co with respect to Au giving a reduced mass thickness contrast for the particles. A range of particle sizes is present, with a maximum of about 4 nm. Especially in this as-quenched material, where the decomposition is a minimum, it is possible that the ion milling stimulated the decomposition through local heating and atom displacements. This may have activated the growth of the particles observed. It is therefore possible that in the samples not prepared for TEM investigations, the Co particles are even smaller.

The subtle dispersion of the particles with a high density throughout the matrix distorts the fcc crystal structure. Nevertheless, due to the absence of Moiré patterns the particles still seem to be largely coherent with the matrix. The microstructure shown in Fig. 2 is homogeneous throughout all of

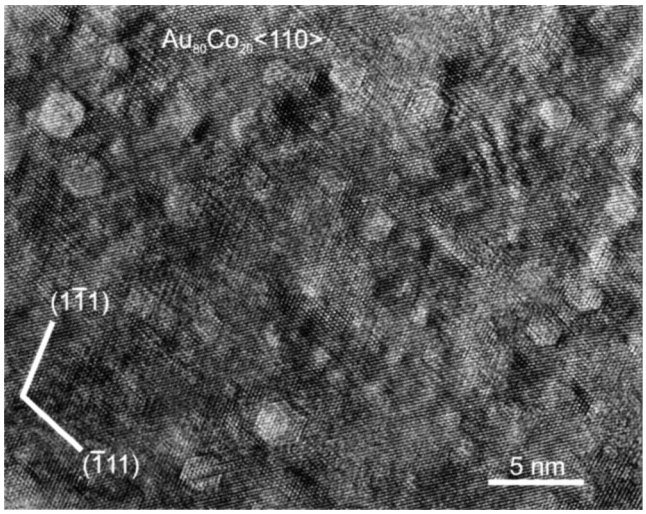

FIG. 2. HRTEM image of as-quenched $Au_{80}Co_{20}$ alloy with well-defined faceted Co particles up to 4 nm in size as viewed along the ⟨110⟩ Au zone axis.

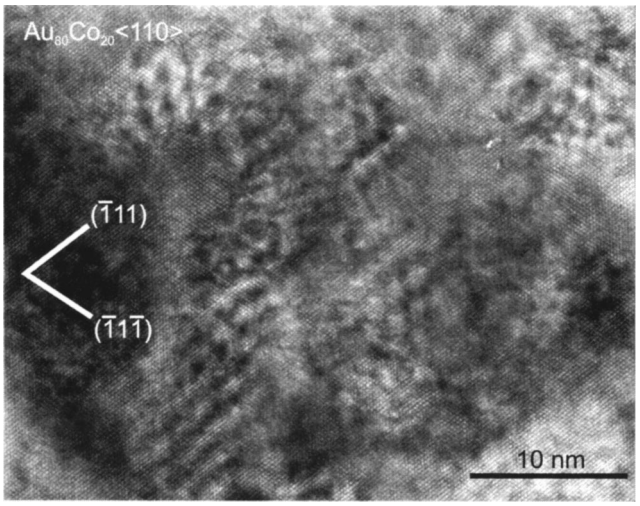

FIG. 3. HRTEM image of $Au_{80}Co_{20}$ alloy annealed 1 h at 400 °C as viewed along the ⟨110⟩ Au zone axis. Spinodal decomposition has caused the particle edges to become diffuse and some particles to become interconnected.

the large Au grains (order of magnitude 100 μm). On the grain boundaries, relatively large Co particles or plates with a size of up to 50 nm are present. Although in this case quenching also did not completely suppress the decomposition, the dispersion of Co throughout the Au is much finer and more homogeneous than in the case of melt spinning. In principle the induced cooling rate during melt spinning is higher than with water quenching. The main difference between the two methods is that the liquid–solid transition occurs during melt spinning, which is absent in the case of solid-solution quenching. Hence, the reason that the microstructure prepared by melt spinning is coarser than that obtained via solid-solution quenching is probably due to the latent heat released. Apparently it slows down the cooling process significantly. Since the nanostructure of the solid-solution quenched material is more suitable for GMR research than that prepared by melt spinning, all GMR and magnetization results were obtained from samples prepared by the former method.

Upon annealing the quenched material we hoped to observe classical growth of the Co particles and then correlate this growth with the change in GMR and magnetic behavior. Indeed, during annealing the Co particles coarsen, but in addition we observed other important effects. At lower annealing temperatures (300 and 400 °C), spinodal decomposition appeared to occur, as became manifest by HRTEM images showing Co particle boundaries that have become diffuse and Co particles that even have become interconnected. An example of a HRTEM image of the sample annealed 1 h at 400 °C viewed along ⟨110⟩ of the Au matrix is shown in Fig. 3. At higher annealing temperature (500 °C for 10 min and 1 h), the system appeared to be above the spinodal and particles with well-defined interfaces were already observed after 10 min of annealing (see Fig. 4). All Co particles observed after annealing possessed the fcc crystal structure and showed parallel topotaxy with the Au matrix. Although the equilibrium phase diagram indicates that below 422 °C hcp is the stable isomorphic structure of Co, hcp Co was never detected upon annealing. The Moiré patterns observed in the TEM images indicate that the Co particles are not coherent with respect to the Au matrix and the interfaces are either in- or semicoherent. Comparing this with the as-quenched structure indicates that annealing introduces loss of coherency between Co and Au.

In the equilibrium phase diagram no (chemical or coherent) spinodal is drawn. Results of calculations of the locus of the chemical and coherent spinodal have been given in Ref. 10 where the coherent spinodal was indicated to be an upper limit. At a composition of 20 at. % Co the locus of the coherent spinodal is at about 200 and 350 °C for assumed isotropic and anisotropic AuCo, respectively, and the locus of the chemical spinodal is at about 600 °C. We observe spinodal decomposition, but certainly not with coherency between Co and Au. Although the temperature where the transition from spinodal decomposition to classical nucleation

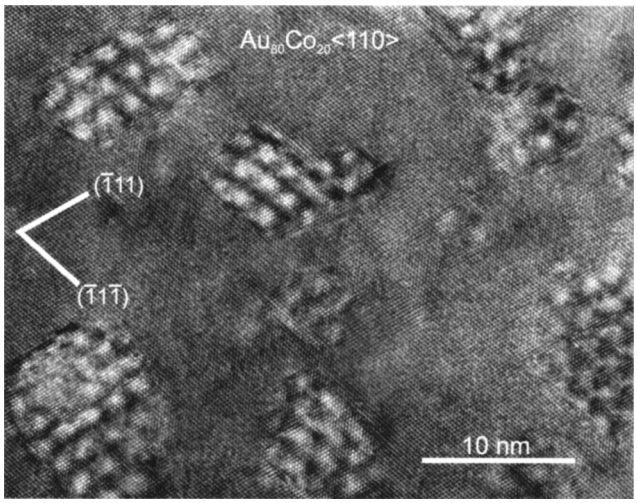

FIG. 4. HRTEM image of $Au_{80}Co_{20}$ alloy annealed 1 h at 500 °C as viewed along the ⟨110⟩ Au zone axis. Particles have grown in size (compare with Fig. 3) and have obtained well-defined interfaces with the Au matrix.

TABLE I. Size of the GMR effect defined by Eq. (1) for the different materials at measuring temperatures of 10 and 300 K at both at 5 and 50 kOe external magnetic-field strength.

	GMR at 10 K		GMR at 300 K	
Alloy heat treatment	5 kOe	50 kOe	5 kOe	50 kOe
As-quenched	6.5%	29%	0.03%[a]	1.7%[a]
1 h at 300 °C	10%	15%	—	—
1 h at 400 °C	6.1%	8.7%	2.4%	3.2%
10 min at 500 °C	1.7%	3.7%	0.94%	1.4%
1 h at 500 °C	1.9%	3.7%	0.96%	1.4%

and growth occurs is difficult to establish experimentally (spinodal decomposition may occur very rapidly, giving rise to sharp interfaces), our results seem to indicate that at 500 °C nucleation and growth are already active. In this respect the calculated spinodals in Ref. 10 appear reasonable in magnitude, but an upper limit indeed.

B. GMR

The variation of resistance R with external magnetic field H for the as-quenched alloy is shown in Fig. 5. As usual, the GMR effect is defined as the ratio

$$\mathrm{GMR}=\frac{R(H)-R(0)}{R(0)}=\frac{\rho(H)-\rho(0)}{\rho(0)}. \tag{1}$$

A better definition that leads more directly to a quantitative understanding of the GMR effect would involve the absolute rather than the relative change in resistivity, i.e., in this way we get rid of the influence of the spin-independent resistivity. However, because accurate measurements of the precise geometry of the thin-foiled specimen during the resistance measurement with four-point probe geometry is rather difficult, the ratio of Eq. (1) is used. The GMR effect is large for a measuring temperature of 10 K: 29% at 50 kOe and still shows a steep decrease and it will clearly become larger for stronger fields. Upon increasing the measuring temperature to 300 K the GMR effect rapidly decreases and almost vanishes.

The annealed samples all behave very differently from the as-quenched alloy, but very similar to each other. A typical curve for the annealed GMR is shown in Fig. 6. Table I provides the relative size of the GMR effect at 5 and 50 kOe for the different materials. The most significant difference between the as quenched and the annealed samples is that the relative decrease in GMR is in the case of the annealed samples clearly larger during the first 5 kOe and smaller for stronger fields. For relatively strong external fields (e.g., 50 kOe) and low temperatures (e.g., 10 K) the GMR effect continuously decreases upon annealing with increasing temperatures. For low field strengths an optimum in GMR effect is present for intermediate annealing temperatures (300–400 °C) independent of the measuring temperature. Finally, for high measuring temperatures (300 K) the GMR effect shows an optimum for intermediate annealing temperatures (300–400 °C) independent of the external field strength. This last results can be attributed largely to the relative reduction of the spin-independent compared to the spin-dependent resistivity upon annealing.

Only Kataoka *et al.*[11] used solid-solution quenching rather than melt spinning to prepare Au–Co alloys for GMR. Remarkably, their article is also the only one in which a relative GMR value comparable to that measured in our as-quenched alloy is reported: 29% at 5 K and 100 kOe for a $Au_{85}Cu_{15}$ alloy.

C. Magnetization

The mass magnetization for the as-quenched alloy is depicted in Fig. 7. It depends strongly on the measuring temperature and does not saturate at any of the measuring temperatures within the field range considered here. Some hysteresis can be observed at low fields at a measuring temperature of 10 K.

Figure 8 shows a typical mass-magnetization curve for the annealed alloys which all show very similar behaviors. There is large hysteresis at low fields at 10 K. Note that the annealed magnetization curves already saturate at about 25 kOe at all measuring temperatures. Calculation of the average moment per Co atom in our annealed samples at saturation yields $1.67\pm0.03\ \mu_B$, while the value given by Ref. 14 is 1.72 μ_B (no measurement uncertainty provided). We can deduce from this fact that one does indeed observe true saturation in our data, rather than an extremely slow approach to saturation with most of the Co still not aligned.

IV. DISCUSSION

Our HRTEM observations reveal a clear distinction between the structure of the alloys annealed at lower (300–400 °C) and those annealed at higher (500 °C) temperatures. The spinodal decomposition that takes place in the former case causes not only growth of the (average) Co particle size, but also fundamentally changes the character of the particles and their interfaces. Spinodal decomposition is not a peculiar phenomenon of the Co–Au system, but can be expected in most systems showing strong decomposition of two phases with endothermic properties. Since for granular GMR materials a very strong tendency for decomposition is essential to arrive at microstructures in which small magnetic clusters develop in a nonmagnetic matrix, this goes hand in hand with a high probability that spinodal decomposition will come into play. Further, we observed for the present alloy that the Co particles are largely coherent in the as-quenched alloy and lose coherency upon annealing. Both these results show clearly that the variation of the GMR with annealing temperature cannot be interpreted as being the result of a simple change in the average Co particle size as is often assumed. Inspection of the real-space structure at the atomic or nanoscale is hence an essential part of the investigation of the influence of annealing on the GMR effect and for establishing the relation between GMR and structure in general.

The GMR data for the annealed samples show hysteresis at all three measuring temperatures. This hysteresis is a combined result of the system properties and the measuring technique. To save helium, the curves of resistance versus exter-

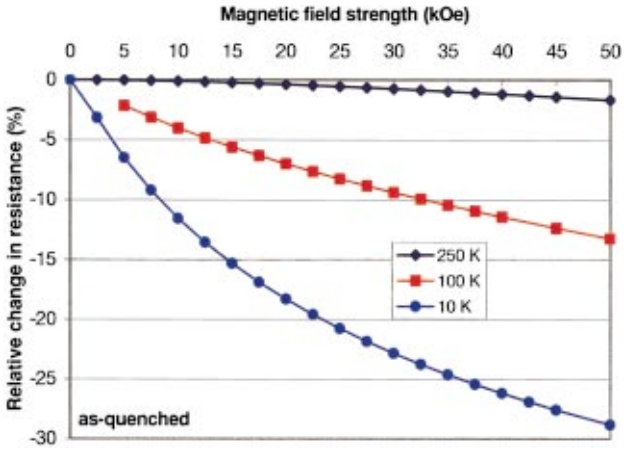

FIG. 5. (Color) Relative change in resistance as a function of external magnetic field for the as-quenched $Au_{80}Co_{20}$ alloy.

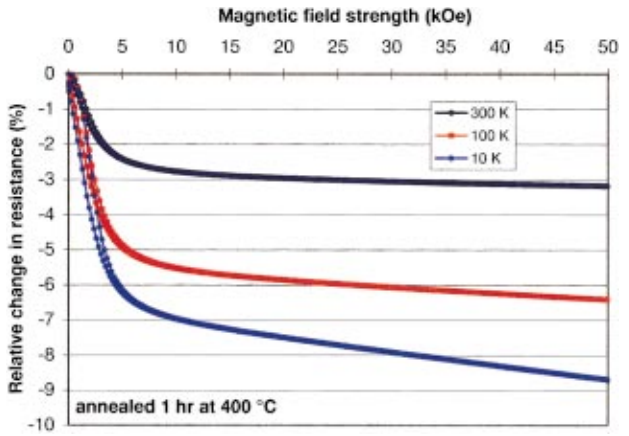

FIG. 6. (Color) Relative change in resistance as a function of external magnetic field for the $Au_{80}Co_{20}$ alloy annealed at 400 °C for 1 h.

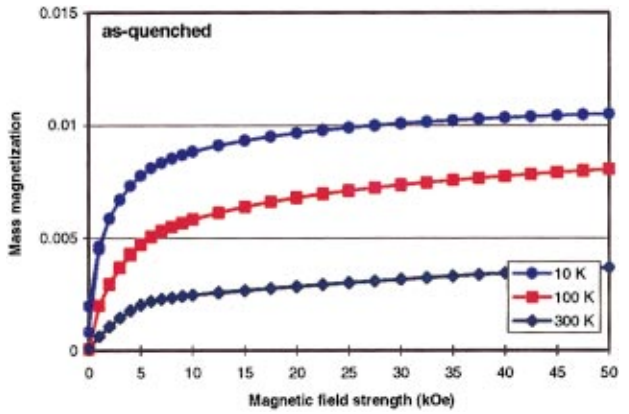

FIG. 7. (Color) Mass magnetization (emu/mg) as a function of external magnetic field for the as-quenched $Au_{80}Co_{20}$ alloy.

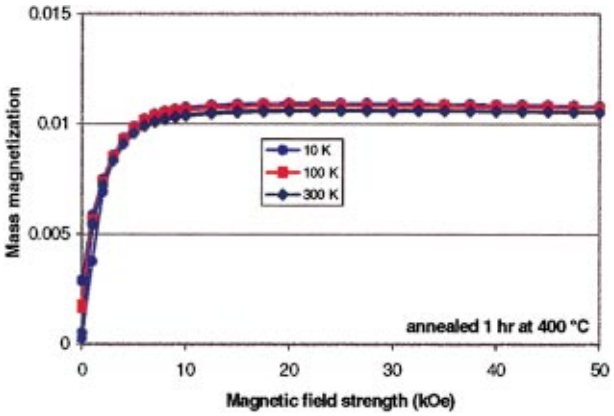

FIG. 8. (Color) Mass magnetization (emu/mg) as a function of external magnetic field for the $Au_{80}Co_{20}$ alloy annealed at 400 °C for 1 h.

nal magnetic field for the annealed samples were measured using a magnetic field that varied slowly and linear in time. Although the magnetic behavior of the annealed samples is *not* bulk SPM (i.e., could not be described by a weighted superposition of Langevin functions), these systems do require time to reach thermal equilibrium similar to SPM behavior. The state of the systems is thus always lagging behind with respect to the actual state of the continuously varying external field at that moment. This probably causes the hysteresis observed between increasing and decreasing

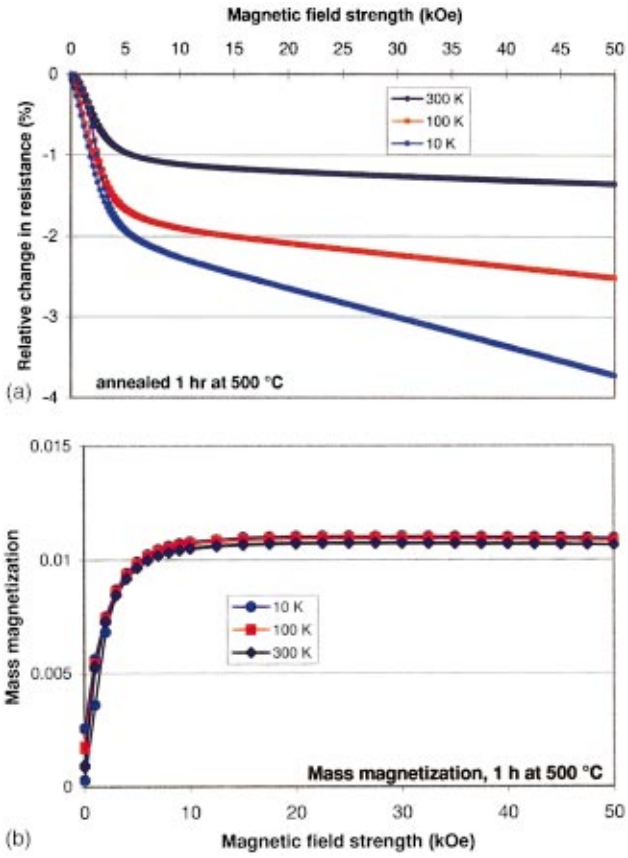

FIG. 9. (Color) (a) Relative change in resistance as a function of external magnetic field and (b) mass magnetization (emu/mg) as a function of external magnetic field for the $Au_{80}Co_{20}$ alloy annealed at 500 °C for 1 h.

fields. The explanation is in accordance with the observation that the hysteresis in the GMR is only measured below ~5 kOe, since only in that region the *R* versus *H* curves are steep enough to yield a measurable influence of the ''lagging-behind'' effect.

The magnetization measurements show a large temperature dependence for the as-quenched alloy. Measurements of the magnetization as a function of temperature confirm the bulk SPM/''blocked'' nature of the behavior. On the other hand, the magnetization of the annealed alloys is virtually independent of temperature, except for the hysteresis behavior at low field strengths and low temperatures. Even though the bulk behavior is not SPM, as can be inferred for example from the temperature independence, apparently there are still some SPM particles in each annealed alloy. When the temperature is lowered from 100 to 10 K, these SPM particles become blocked and their magnetization then exhibits hysteresis at low fields. The behavior of the as-quenched material is in reasonable correspondence with the model put forward by Wiser[5] and Musa *et al.*[6] Indeed, there is a qualitative similarity between both the magnetization and the GMR curves of the present work and the corresponding curves in their work. From these similarities and our magnetization data we conclude that the as-quenched alloy contains a collection of SPM and blocked particles, where their fractions vary with temperature. Our inspection of the microstructure confirms that this is possible: the cobalt particles, present in a distribution of sizes, are well separated and small enough to be single domain. The GMR could then be expressed as a function of the magnetization.

For annealed alloys, we encounter a fundamental difficulty when trying to compare our data to any model that relates the GMR to the overall magnetization. This problem is clearly illustrated if Figs. 9(a) and 9(b) are compared. These figures show the GMR and magnetization, respectively, as a function of the magnetic field for the sample annealed 1 h at 500 °C. At high fields above (~20 kOe), the magnetization saturates while the GMR shows a steady decrease. Therefore, at fields above ~20 kOe, the GMR can impossibly be a function of the overall magnetization for the annealed alloys. This combination of saturating magnetization and steadily decreasing resistance can already be observed in Ref. 2 and has also been presented by other researchers.[7,15,16] The phenomenon has received only scant attention and there has not been an attempt to arrive at a thorough explanation. In all cases, it appears that at high fields extremely small changes in the magnetization still induce large changes in the resistance. The GMR, hence, cannot be a mathematical function of purely the overall magnetization.[17]

A possible explanation is the alignment at high fields of extremely small SPM particles, or of paramagnetic CO atoms, possibly located in the diffuse-boundary regions or at the boundaries of Co particles. Because of the saturating magnetization, these particles or atoms can only constitute a very small amount of Co and hence are very limited in number. This means that the resistivity would have to be extremely sensitive to changes in the direction of the magnetic moments of these particles or atoms. The combination of saturating magnetization and steadily decreasing resistance is a challenging effect. Understanding its origin may lead to a better understanding of the GMR effect as a whole.

An interesting observation is that although the observed microstructures of the alloys annealed above and below the spinodal are very different, their magnetic and magnetoresistive behavior are quite similar. Both the magnetization and the GMR curves have similar shapes for all annealed samples and actually only the relative size of the effect really makes the difference. In contrast, the magnetization and GMR curves for the as-quenched alloy have very different shapes (compare Figs. 5 with 6 and Figs. 7 with 8). The most important difference between the as-quenched and the annealed alloys is (apart from the coarsening) that the Co particles in the former case are still largely coherent, whereas in the latter case they have lost coherency (despite the diffuse boundaries in the case of spinodal decomposition). The spin-dependent transport is therefore probably rather sensitive with respect to the coherency of the magnetic Co particles inside the nonmagnetic Au matrix and not sensitive to the sharpness of the interfaces themselves. Spin-dependent scattering at the magnetic particle interfaces is often considered to give a major contribution to the GMR [e.g., 3, 19–21]. Therefore, loss of coherency across these interfaces can be expected to have a possibly strong effect on the GMR behavior as is confirmed by the present observations.

V. CONCLUSIONS

Melt spinning $Au_{80}Co_{20}$ (with a velocity at the surface of a Cu wheel of 30 m/s) resulted in a rather inhomogeneous nanostructure, already too coarse to be of real interest for GMR properties. On the other hand, solid-solution annealing followed by water quenching appeared to be a suitable method for the preparation of giant magnetoresistive granular gold–cobalt alloys: we have measured a GMR of 29% at 10 K and 50 kOe. The bulk behavior of this alloy is compatible with the presence of a collection of Co particles with a size distribution: the smaller ones being SPM and the larger ones being blocked. Inspection of the microstructure with HRTEM reveals that a range of sizes is indeed present.

Subsequent annealing at 300 and 400 °C fundamentally changes the Co particles through spinodal decomposition and loss of coherency between the Co- and Au-rich phases. The particle boundaries become diffuse and the particles even become interconnected. These effects illustrate that the influence of annealing should always be investigated by checking the microstructure directly, rather than inferring a simple change in the average particle size from magnetic or resistance data.

The annealed alloys show the remarkable coincidence of saturating magnetization and steadily decreasing resistance. For these alloys, the GMR can impossibly be a function of the overall magnetization. If the decrease of resistance at high fields is attributed to small SPM particles or paramagnetic Co atoms, the GMR should be extremely sensitive to changes in the orientation of their magnetic moments to achieve the measured effect. Apparently magnetic alignment of sites for spin-dependent scattering does not significantly

influence the overall magnetization, but is still of considerable importance for the resistance. Possibly these sites are located at the (diffuse) Au/Co interfaces.

The marked difference between the GMR and magnetization properties of the as-quenched and the annealed alloys is probably related to the loss of coherency of the Co with respect to the Au upon annealing (without much influence of the spinodal decomposition) as was revealed by HRTEM. The state of coherency of the small magnetic clusters inside the nonmagnetic matrix apparently strongly affects the spin-dependent transport that is at the basis of the GMR effect.

ACKNOWLEDGMENTS

The assistance of Dr. P. M. Bronsveld with the use of the arc furnace and with melt spinning is gratefully acknowledged. The authors want to thank in particular Professor T. T. M. Palstra for providing them with the opportunity to use his equipment for GMR and magnetization measurements and for his assistance during the experiments and for discussion. They also thank J. Baas for technical assistance with the GMR and magnetization measurements.

[1] S. Zhang, F. E. Spada, F. T. Parker, A. Hütten, and G. Thomas, Phys. Rev. Lett. **68**, 3745 (1992).
[2] J. Q. Xiao, J. S. Jiang, and C. L. Chien, Phys. Rev. Lett. **68**, 3749 (1992).
[3] S. Zhang and P. M. Levy, J. Appl. Phys. **73**, 5314 (1993).
[4] A. Vedyayev, B. Mevel, N. Ryzhanovam, M. Tshiev, B. Dieny, A. Chamberod, and F. Brouers, J. Magn. Magn. Mater. **164**, 91 (1996).
[5] N. Wiser, J. Magn. Magn. Mater. **159**, 119 (1996).
[6] J. F. Gregg, S. M. Thompson, S. J. Dawson, K. Ounadjela, C. R. Staddon, J. Hammon, C. Fermon, G. Saux, and K. O'Grady, Phys. Rev. B **49**, 1064 (1994).
[7] P. Allia, M. Knobel, P. Tiberto, and F. Vinai, Phys. Rev. B **52**, 15398 (1995).
[8] S. O. Musa, M. A. Howson, B. J. Hickey, and N. Wiser, J. Magn. Magn. Mater. **148**, 309 (1995).
[9] J. Bernardi, A. Hütten, S. Friedrichs, C. E. Echer, and G. Thomas, Phys. Status Solidi A **147**, 65 (1995); A. Hütten, J. Bernardi, C. Nelson, and G. Thomas, *ibid.* **150**, 171 (1995).
[10] A. Hütten, J. Bernardi, S. Friedrichs, G. Thomas, and L. Balcells, Scr. Metall. Mater. **33**, 1647 (1995).
[11] N. Kataoka, H. Takeda, J. Echigoya, K. Fukamichi, E. Aoyagi, Y. Shimada, H. Okuda, K. Osamura, M. Furusaka, and T. Goto, J. Magn. Magn. Mater. **140–144**, 621 (1995).
[12] *LR-700 AC Resistance Bridge User's Manual*, Version 1.2 (Linear Research Inc.).
[13] *Magnetic Property Measurement System Hardware Reference Manual* (Quantum Design, Inc., San Diego, CA, 1990).
[14] B. D. Cullity, *Introduction to Magnetic Materials* (Addison-Wesley, Reading, MA, 1972).
[15] R. von Helmot, J. Wecker, and K. Samwer, Appl. Phys. Lett. **64**, 791 (1994).
[16] A. Maeda, M. Kume, S. Oikawa, and K. Kuroki, J. Appl. Phys. **76**, 6793 (1994).
[17] A. Tsoukatos, D. V. Dimitrov, A. S. Murthy, and G. C. Hadjipanayis, J. Appl. Phys. **76**, 6799 (1994).
[18] S. A. Makhlouf, K. Sumiyama, K. Wakoh, K. Suzuki, K. Takanashi, and H. Fujimori, J. Magn. Magn. Mater. **126**, 485 (1993).
[19] J. Inoue, J. Magn. Magn. Mater. **164**, 273 (1996).
[20] P. Baumgart, B. A. Gurney, D. R. Wilhoit, T. Nguyen, B. Dieny, and V. S. Speriosu, J. Appl. Phys. **69**, 4792 (1991).
[21] S. S. P. Parkin, Phys. Rev. Lett. **71**, 1641 (1993).